THE JOURNAL OF PHYSICAL CHEMISTRY A
Article
Cite This: J. Phys. Chem. A XXXX, XXX, XXX−XXX
pubs.acs.org/JPCA

What Electronic Structure Method Can Be Used in the Global Optimization of Nanoclusters?

Breno R. L. Galvão*[,†] and Luís P. Viegas*[,‡,§]

[†]Centro Federal de Educação Tecnológica de Minas Gerais, CEFET-MG, Av. Amazonas 5253, 30421-169 Belo Horizonte, Minas Gerais, Brazil

[‡]Aarhus Institute of Advanced Studies, Aarhus University, Aarhus DK-8000, Denmark

Supporting Information

ABSTRACT: The problem of obtaining the spatial structure of nanoclusters is known to be very difficult due to the large number of local minima associated with their potential energy surfaces (isomers). In global optimization approaches, such as basin hopping and genetic algorithms, the problem is normally tackled by first using a low-level and affordable method to evaluate the energy. Afterward, the putative global minimum (and often a few others) is refined with calculations using higher level methods and larger basis sets. There is no guarantee, however, that the structure obtained at the lower level method will be the global minimum at the refined one. In this work, we have performed benchmark coupled cluster calculations at the complete basis set limit for a large number of different isomers of representative clusters of third row elements. Such calculations are then employed to check the hypothesis that lower level methods can be used in the global optimization with reliable results. For this, we have developed a methodology that allows us to compare a large number of minima obtained at different calculation levels. The results indicate that, if the global optimization is capable of reaching not only the global minimum but also a reduced number of low lying structures, most of the tested density functional theory (DFT) functionals are good choices, with emphasis on TPSSh. Besides giving a more solid ground to this commonly used approach, this work helps guiding such global optimizations. The use of the MP2 method and several scaled variants is also assessed, from where it is concluded that the scaled variants yield better results than standard MP2 or DFT approaches, except for one system where a large number of van der Waals structures exist.

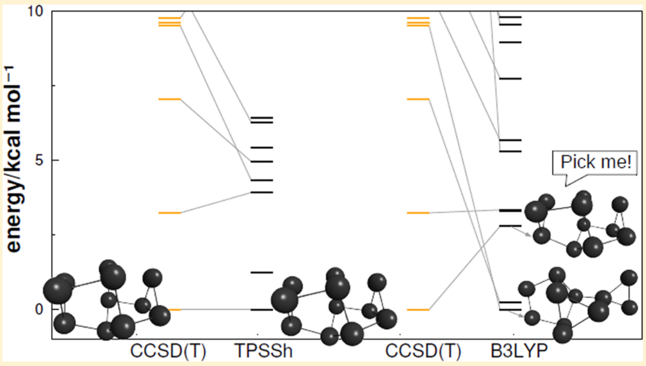

1. INTRODUCTION

The study of aggregates of atoms in the nanoscale and subnanoscale has the potential of creating materials with very unusual physicochemical properties that may eventually lead to specific applications for areas as distinct as medicine and catalysis.[1,2] Experimental works have flourished in the past decades, while computer-aided interpretation of the results and predictions of new possibilities has advanced together in a complementary fashion.[3]

A major step in such theoretical studies is the determination of the structure of the global minimum (GM) associated with the potential energy surface (PES) of these clusters, which will be most likely produced in an experiment. This search for the GM structure is very difficult since the number of degrees of freedom allows for the existence of thousands of local minima. Chemical intuition often fails in this problem, and direct experimental measurement of a cluster's geometry is not currently possible. However, if trustworthy theoretical predictions are possible, they may be used for accurate predictions of relevant properties, which in turn may be useful for guiding the design of new nanoclusters with interesting applications. For this reason, a deep understanding of the reliability concerning the theoretical results is of fundamental importance.

Accurate ab initio calculations become quickly prohibitive as the number of atoms and electrons increases. For example, the computational cost of coupled-cluster calculations scales as $O(o^2v^4)$, where o and v are the number of occupied and virtual orbitals, respectively. This poses a serious limit on the size of clusters that may be treated with such methods using current computers. The normal approach is to perform global optimizations[4−6] using a low-level calculation and to select one (or a few) low-energy isomer for local reoptimization with a more accurate ab initio method.[3,7−23] However, there is no guarantee that the GM of the low-level method will correspond to the "real" structure, and although this is a reasonable approach, it is largely untested. In this work, we perform benchmark CCSD(T)[24−27] calculations over a large number of energy minima in the PESs of selected clusters to shed light on the viability of such an approach and to test which lower level

Received: October 2, 2019
Revised: November 8, 2019
Published: November 8, 2019

DOI: 10.1021/acs.jpca.9b09309

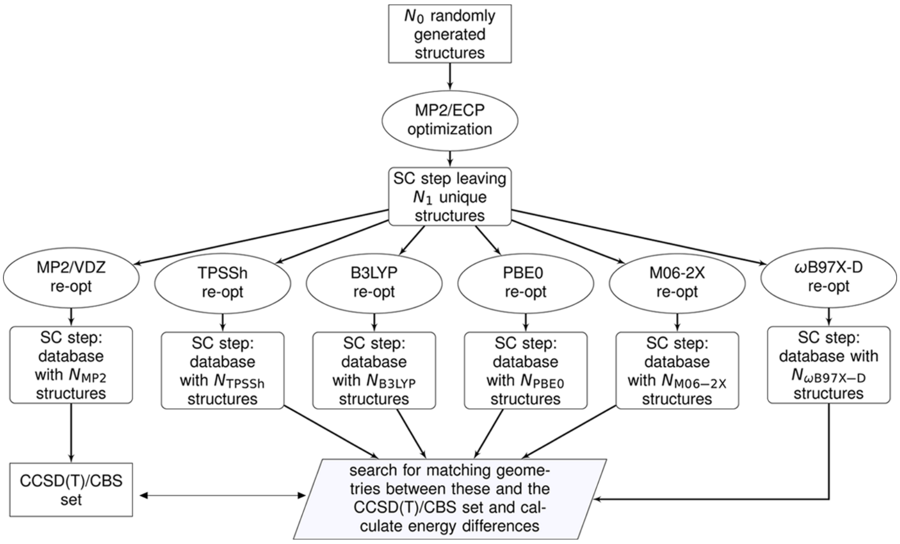

Figure 1. Flowchart for the generation of the databases employed in this work for homonuclear clusters. The ellipses are used to indicate geometry optimizations within a given database, and rectangles with rounded corners indicate the removal of equivalent geometries (see text).

calculation is more suited for the exploratory part. To this endeavor, we employ clusters of different natures (alkali, metallic, and covalent) spanning a large portion of third row elements and including alloys and cationic species. The benchmark results consist of CCSD(T) calculations extrapolated to the complete basis set limit, and for this reason, only third row elements were chosen as this approach becomes prohibitive for heavier atoms.

2. METHODS

2.1. Electronic Structure Calculations. Several electronic structure methods have been employed in this work. Among the wave function-based methods, we utilized the second-order Møller−Plesset perturbation theory (MP2[28]) with the cc-pV(*D*+*d*)Z (or simply V*D*Z) basis set[29] (hereafter indicated as MP2/V*D*Z) and also with the LANL2DZ basis set with an effective core potential[30−32] (indicated as MP2/ECP). The energy of three scaled variants of the MP2 method was also used for comparison, namely, the spin-component scaled (SCS-MP2[33]), scaled opposite-spin (SOS-MP2[34]), and variable-scaling opposite-spin (VOS-MP2[35]).

For benchmarking purposes, single-point coupled-cluster singles and doubles plus perturbative triples[24−27] (CCSD(T)) calculations have also been performed with the V*D*Z and cc-pV(*T*+*d*)Z (V*T*Z) basis sets.[29] This pair of calculations was used for extrapolation to the complete basis set (CBS) limit with the USTE method[36] adapted with re-hierarchization of the basis set.[37] Within this method, the Hartree−Fock (HF) and dynamical correlation energies are extrapolated separately, with the HF limit ($E^{\mathrm{HF}}_{\mathrm{CBS}}$) obtained by[38]

$$E^{\mathrm{HF}}_{\mathrm{CBS}} = E^{\mathrm{HF}}_{x_2} + \frac{e^{\beta x_1}}{e^{\beta x_2} - e^{\beta x_1}}(E^{\mathrm{HF}}_{x_2} - E^{\mathrm{HF}}_{x_1}) \tag{1}$$

where $E^{\mathrm{HF}}_{x_1}$ is the total HF/V*D*Z energy and $E^{\mathrm{HF}}_{x_2}$ is the V*T*Z one. Instead of using the usual cardinal numbers ($X = 2, 3$) for these two basis sets, those after re-hierarchization are employed ($x_1 = 2.08$ and $x_2 = 2.96$), while the parameter β is fixed at 1.62. All such values were calibrated in ref 38. The extrapolation of the correlation energy (cor) is obtained by[37]

$$E^{\mathrm{cor}}_{\mathrm{CBS}} = E^{\mathrm{cor}}_{x_2} + \frac{x_1^3}{x_2^3 - x_1^3}(E^{\mathrm{cor}}_{x_2} - E^{\mathrm{cor}}_{x_1}) \tag{2}$$

where again hierarchic numbers were employed for this type of calculation, namely, $x_1 = 1.91$ and $x_2 = 2.71$, according to ref 37.

As for calculations within the density functional theory (DFT) approach, we have used the TPSSh,[39] B3LYP,[40−42] PBE0,[43,44] M06-2X,[45] and *ω*B97X-D[46] fourth rung[47,48] functionals, always in conjunction with the polarization consistent basis set pcseg-1.[49] We have also attempted optimizations with several third rung functionals, but converging the SCF cycles was many times found to be impossible, so we discarded their use. All calculations presented in this work were performed with the GAMESS[50] package and using restricted methods.

2.2. Similarity and Dissimilarity Checks. In this work, hundreds of geometrical structures are optimized, and symmetrically equivalent ones are obtained frequently. For this reason, a method for identifying equivalencies is necessary. Furthermore, we wish to compare similar isomers obtained by local optimizations with different methods (such as between MP2 and DFT results), and we need a criterion to determine if their geometries can be considered corresponding to one another, despite small differences in bond lengths that will naturally occur between the two methods. This could be performed visually, which would be a hard task for a few pairs of structures of moderate size, but here we perform thousands of such comparisons, and therefore an automatic algorithm is of fundamental importance.

For this, each necessary pairwise comparison[51] is done using a superimposing algorithm[52] that quantifies the dissimilarity (*d*) between the two structures by minimizing the sum over all distances between each corresponding atom. This algorithm has been upgraded to identify enantiomers,[53] and we use this latter implementation in this work (which is particularly useful for alloys).

Whenever we want to identify identical structures within a database of a given method, we will proceed with a similarity check (SC), by which we mean a pairwise comparison between all structures followed by removing those deemed as identical

DOI: 10.1021/acs.jpca.9b09309

(here we consider $d < 0.05$ Å). On the other hand, when a matching between similar structures obtained with different methodologies is needed, the comparison will allow larger values of d.

2.3. Generation of Structure Databases. For obtaining a large number of unique structures for homonuclear clusters and compare the PESs of different quantum chemical methods, we have elaborated a new scheme, which is outlined schematically in Figure 1. First, we generate a large number (N_0) of random geometries (using the procedure outlined in ref 54), which were optimized at the MP2/ECP level. This is followed by an SC step to remove equivalent ones, which leads to a reduced set of N_1 unique structures. This first relaxation with such a low-level method is simply to generate reasonable geometries and avoid optimizing equivalent minima with higher level methods.

This preliminary database is reoptimized separately with several higher level methods, and frequency calculations are always performed to guarantee that a true minimum has been obtained. The first approach is again MP2 but without an effective core potential (MP2/V*DZ*). Although the MP2 method is not the standard choice for global optimizations, it has recently also been used for some small clusters.[54,55] At this point, the reoptimizations lead to new equivalencies in the database (not present in the N_1 set), and another SC step is performed to avoid this possibility. This new set of structures will have N_{MP2} minima, and for these we also save the energies of the SCS-MP2, SOS-MP2, and VOS-MP2 variants without further optimizations. For the SCS-MP2 case, for example, the energies could be indicated as SCS-MP2/V*DZ*//MP2/V*DZ*. Note that, in many cases, these MP2 variants are known to outperform standard MP2 and yield results of coupled-cluster type quality.[33,35,56]

The most popular choice for theoretical calculations on nanoclusters is of course DFT, and therefore the initial structures from the preliminary N_1 database were optimized (and frequency calculations performed) with four different fourth rung[47,48] functionals: TPSSh[39] ($a_0 = 0.10$), B3LYP[40−42] ($a_0 = 0.20$), PBE0[43,44] ($a_0 = 0.25$), and M06-2X[45] ($a_0 = 0.54$) using the pcseg-1 basis set.[49] Note that these functionals were chosen such as to span different fractions of Hartree−Fock exchange (a_0). A dispersion-corrected functional[57] (ωB97X-D) is also included in the final list. A new SC step is performed, and each functional will now have a different set with N_{TPSSh}, N_{B3LYP}, N_{PBE0}, $N_{\mathrm{M06\text{-}2X}}$, and $N_{\omega\mathrm{B97X\text{-}D}}$ different energy minima. Consequently, the geometry in each functional is optimized independently, and the results may be written as DFT/pcseg-1//DFT/pcseg-1. Finally, for the functional with best results, we also test a very attractive cost-effective method by generating a database using an ECP instead of the pcseg-1 basis set since an accurate application of the DFT/ECP methodology would represent a drastic decrease in computing time.

Our benchmark energies will consist of CCSD(T)/CBS single-point calculations performed at the MP2/V*DZ* geometries (which can be described as CCSD(T)/CBS//MP2/V*DZ* and only shown as CCSD(T) in the figures for simplicity), and the quality of the energies obtained by the other methods will be compared to them. The geometries and energies of these benchmark sets are given in the Supporting Information. A difficulty that arises here is how to compare the energy of a local minimum optimized using DFT calculations with another at the benchmark database (since their geometries are not identical and a match between them is not obvious). For example, if a planar and a pyramidal minimum exist for a given X_n cluster at the benchmark database, it is quite probable that corresponding minima exist at the DFT PES, although they would not be identical due to small differences in bond lengths and angles. Clearly, one could match them by visual inspection, but this would be a very hard task for large clusters, and this pairwise comparison would be necessary hundreds of times. For creating connections between corresponding minima at two distinct levels, we have developed an algorithm to compare all possible pairs of structures in two databases and calculate their dissimilarity d. We have tried different cutoff values and found that $d < 0.6$ yields correct results when compared to eye inspection. It is sometimes the case that a given DFT minimum cannot be matched to any minima in the benchmark database, and thus it cannot be used in the comparisons. Therefore, if only the matched isomers are considered, the number of structures in the databases will be indicated with primed variables (N'_{TPSSh}, N'_{B3LYP}, N'_{PBE0}, $N'_{\mathrm{M06\text{-}2X}}$, and $N'_{\omega\mathrm{B97X\text{-}D}}$).

In the case of alloys, the number of energy minima is drastically increased because, for each geometrical shape that may be assumed by the cluster, all permutations of nonequivalent atoms also result in another isomer (the term homotop is used for this kind of isomerism[58]). In such cases, the scheme presented in Figure 1 is not used for the creation of the databases. Instead of randomly generating the several energy minima, we start with a given known geometry (corresponding to a known energy minima of the system) and generate all possible permutations from it by performing all possible atom swap moves. Before optimizing the obtained set of geometries, we first delete any equivalent permutations (due to symmetry). After the optimizations of such structures on all levels of theory, new equivalences (or enantiomers) may be further achieved, and thus an SC step is also performed here for each method independently, which yields the different databases. It must be emphasized that, in the case of alloys, several enantiomers are available, which are hard to detect by eye inspection, and the algorithm employed here[53] is particularly appropriate.

The energies are reported relative to the GM of each method. Another obvious choice would be the total binding energy, which would also give a good estimate on how well each approach compares with the benchmark on this relevant property. However, since our main goal here is to provide good methods for global optimization runs, and not a method that provides accurate binding energies (this is better left for the refinement step, after the global optimization has been performed), we have chosen to set the energy zero of each method at its putative global minimum.

3. RESULTS

3.1. Al_{12}. Aluminum clusters have been much studied due to their potential applications in microelectronics.[59] Several global optimization studies (see refs 8 and 11 and references therein) have been performed for neutral and ionic species, and here we focused on the Al_{12} case.

From the $N_0 = 500$ random structures optimized in the preliminary set, only $N_1 = 108$ were unique, and the rest was discarded after a first SC. As mentioned in Section 2.3, these 108 structures were further optimized with seven distinct methods (MP2/V*DZ*, five DFT functionals with the pcseg-1 basis set, and one functional with ECP basis), thus generating

DOI: 10.1021/acs.jpca.9b09309
J. Phys. Chem. A XXXX, XXX, XXX−XXX

seven databases for the Al_{12} cluster. Note that the number of structures in these databases is less than 108 due to the appearance of new equivalencies after the SC step. Following the nomenclatures given in Figure 1, we have $N_{\mathrm{MP2}} = 44$, $N_{\mathrm{TPSSh}} = 53$, $N_{\mathrm{B3LYP}} = 53$, $N_{\mathrm{PBE0}} = 55$, $N_{\mathrm{M06\text{-}2X}} = 62$, and $N_{\omega\mathrm{B97X\text{-}D}} = 40$.

In order to assess the accuracy of each method in representing the PES of the cluster, we proceeded with the matching of their structures and energies against those of the CCSD(T)/CBS database. These benchmark calculations took 496 days of single CPU time, and the benchmark GM structure is in agreement with the results from the literature using genetic algorithms.[8,11] The results can be seen graphically in Figure 2, which shows the energies of the minima obtained in each method as horizontal bars, with gray lines connecting corresponding geometries. A good match between the PES of a given method and the benchmark one would be seen as fairly straight lines, with few crossings between them. The graphic shows only a limited energy range to allow for a better comprehension of the connections. The full figure can be found in the Supporting Information. Any crossing between two lines represents a different energetic ordering between the two methods. Furthermore, there are unmatched points between the sets, which correspond to unique minima in a low-level method that do not correspond to any minima on the benchmark database according to our criterion. If they share the global minimum structure, the lowest line will be perfectly horizontal at zero energy. If they have different structures as global minima, the lowest lines will have a nonzero slope and we quantify this difference by defining the variable ΔGM_X, which is the energy difference between the GM of a given method X and the isomer that would correspond to the correct global minimum. If the low-level method X and the benchmark one show the same structure as GM, this variable will be zero. This is the main feature of the comparison for determining if a given method could be used in a global optimization, from which only its lowest energy minimum will be extracted and perhaps refined with higher level calculations. It can be seen that no DFT functional is successful in this aspect, and only MP2 optimizations with single-point energies from its scaled variants could be used in such a global optimization.

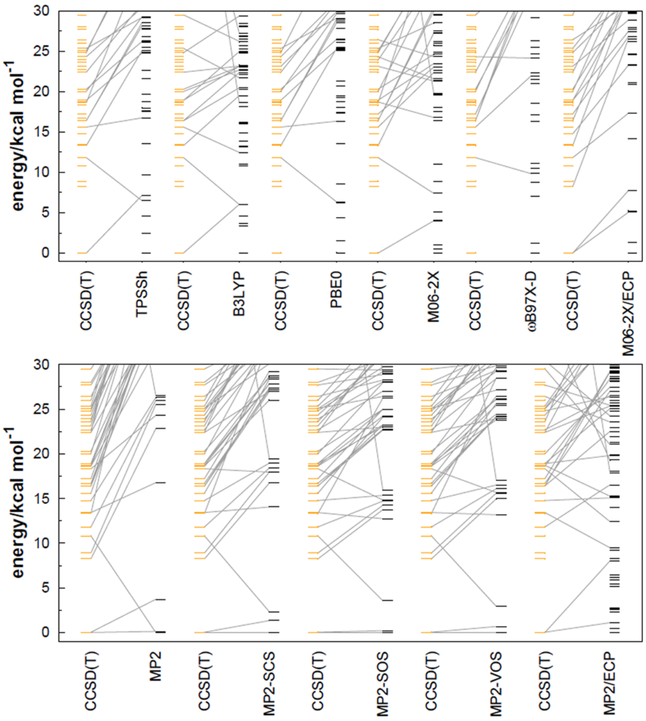

Figure 2. Comparisons between the minima of Al_{12} with several low-level approaches (black bars) against the benchmark CCSD(T)/CBS calculations (orange). The gray lines connect two similar minima on the different approaches (see Section 2.2). A given structure on one method may not find a corresponding one in the other set, which explains the unconnected bars. Each bar is connected only once in a one-to-one fashion, although nearly degenerate structures may appear otherwise. A plot showing the full energy range and all minima obtained can be found in the Supporting Information.

If the low-level method X fails to predict the same GM as the benchmark one, a global optimization using X could still be successful if it could predict not only its putative global minimum but also a few other lowest energy structures for refinement. In the context of this work, refinement implies using the final optimized geometries of the low-level method as starting geometries for the benchmark procedure. As mentioned before, such methodology is widely used in global optimization approaches. For example, as it can be seen in Figure 2, the structure obtained as GM using the TPSSh functional does not correctly predict the benchmark one, but if the global optimization could provide the five lowest energy minima of the TPSSh PES for further refinement at the benchmark level, the refinement process would change the energy ordering and yield the correct one. Thus, besides reporting ΔGM, we also provide in Table 1 the number of structures to be refined (NSR) that would be required for a successful utilization of the low-level method in a global optimization for this system.

Table 1. Summary of the Results for Al_{12}[a]

method	# matches	MAE	ΔGM[b]	NSR[c]
TPSSh	16	8.59	7.15	5
B3LYP	16	8.21	NM[d]	
PBE0	14	7.94	NM[d]	
M06-2X	22	9.54	4.01	4
ωB97X-D	11	10.37	NM[d]	
M06-2X/ECP	21	10.14	7.74	7
MP2	43	17.73	0.13	2
SCS-MP2	43	10.20	0.00	1
SOS-MP2	43	6.72	0.00	1
VOS-MP2	43	7.76	0.00	1
MP2/ECP	32	8.26	7.99	15

[a] Energies are given in kcal mol^{-1}. [b] Energy difference between the GM of a given method and the isomer that corresponds to the correct GM in the benchmark level. [c] Number of structures to be refined for a successful utilization of the global optimization method employing the low-level calculation. [d] No match (NM): the global minimum at the benchmark level has no matching structure at this approach.

Not all minima in one method corresponds to a minimum in the benchmark database, and the number of matches that could be attributed (gray lines in Figure 2) is also given in Table 1, being an indication of how well does the low-level method represent the whole of the benchmark PES. Finally, if more than one low-level method is deemed appropriate for a global optimization (predicts the correct GM and has many matches with the benchmark), one may choose among them

DOI: 10.1021/acs.jpca.9b09309
J. Phys. Chem. A XXXX, XXX, XXX−XXX

Table 2. Results for Na_{10} and Mg_{10}[a]

	Na				Mg			
method	# matches	MAE	ΔGM	NSR	# matches	MAE	ΔGM	NSR
TPSSh	9	0.36	0.57	2	12	5.26	0.00	1
B3LYP	5	0.36	0.00	1	9	15.59	0.00	1
PBE0	7	0.28	0.24	2	11	7.07	0.00	1
M06-2X	5	0.26	0.30	2	11	13.32	2.33	2
ωB97X-D	4	1.33	0.00	1	7	10.63	0.00	1
MP2	13	0.37	0.25	2	16	11.27	1.45	3
SCS-MP2	13	0.12	0.00	1	16	4.07	0.00	1
SOS-MP2	13	0.23	0.00	1	16	1.31	0.00	1
VOS-MP2	13	0.16	0.00	1	16	1.73	0.00	1
MP2/ECP	11	0.43	0.50	3	14	11.38	0.00	1

[a] Energies are given in kcal mol^{-1}.

by using the mean absolute error (MAE) of method X defined as

$$\mathrm{MAE}_{\mathrm{X}} = \frac{\sum_{i=1}^{N'_{\mathrm{X}}} |E^{i}_{\mathrm{CCSD(T)/CBS}} - E^{i}_{\mathrm{X}}|}{N'_{\mathrm{X}}} \tag{3}$$

where N'_X is the number of structures obtained with method X that have a match in the benchmark set. The energies are relative to the GM of each method as in the figures. This is also given in Table 1.

From the results of Figure 2 and Table 1, it can be seen that only the MP2 scaled variants could be employed with success in a standard global optimization run since they have the same GM structure of the benchmark PES. The best choices would be the SOS-MP2 and VOS-MP2 methods since they show the lowest MAEs. Among the DFT functionals, only TPSSh and M06-2X could be used to determine the correct GM (within our approximation) provided that the five lowest lying structures are obtained. The B3LYP functional predicts the second lowest lying coupled-cluster structure, which is nearly degenerate with the GM, but it does not predict the GM itself. The other functionals also do not show a structure that could be matched with the benchmark GM. The best choice for a functional would be M06-2X, which showed more matching structures, lower GM, and only four structures necessary to yield the correct GM (NSR). We also checked if this functional would still be a good choice with a reduced ECP basis set, and although making the results worse, perhaps this would be a reasonable choice if the pcseg-1 basis set becomes prohibitive. With an NSR of 15, the use of ECP with the MP2 method is shown to provide much worse results, thus not being a good choice for a global optimization of Al_{12}.

3.2. Na_{10} and Mg_{10}.

After the seminal experiments performed by Knight et al.,[60] which showed the existence of magic numbers in the mass spectra, sodium clusters have been considered prototypical for both theoretical and experimental works. Magnesium clusters have also attracted attention due to its size-induced transition to metallicity.[61] Using the same framework described above, we explored the PESs of Na_{10} and Mg_{10}. These were simpler problems since the number of existing energy minima is much smaller than for Al_{12}. In fact, from the N_0 = 500 random structures optimized in the preliminary set, only N_1 = 36 were found to be unique after a first SC (reoptimization with method X further reduces this number to N_X; see Figure 1).

The results are given in Table 2, where it can be seen that for these two clusters the scaled variations of the MP2 method would also be the safest choices (ΔGM = 0 and NSR = 1) for both Na_{10} and Mg_{10} with a very low MAE. The B3LYP functional was also capable of achieving this result, although showing the highest MAE. Perhaps the best news from this part was that all methods could obtain the same GM structure as the benchmark provided that three (a modest number) lowest minima in each method were obtained and refined at the high-level method.

3.3. Al_4Si_7.

Alloys are known to display a much larger number of minima than pure clusters of the same size, and we have also included one such example in our explorations. However, as described in Section 2.3, the generation of a database was not based on the random process as in the previous cases. For Al_4Si_7, we start from one single structure (the putative GM obtained in ref 55) and generate all possible atom permutations (11!/(4!7!) = 330) for reoptimization with the different methods (no preliminary optimizations were necessary since the structures are not random). Note that, in this case, we are not exploring the whole PES, but the number of matching structures is large because Al and Si have similar radii and the atom permutation moves do not drastically change the shape of the minima.

Since the original structure shows a plane of symmetry, several permutations may lead to equivalent minima. A first SC step is performed in all generated homotops before optimization, and the number of unique structures was reduced to 185. These are then optimized with each method here employed, which leads to new equivalencies and a different number of structures for each method: MP2/ECP:72, MP2/VDZ:74, B3LYP:80, PBE0:79, TPSSh:76, and M06-2X:78.

The CCSD(T) calculations used in the extrapolation took 268 days in single CPU time, and the CBS extrapolated results are shown in Figure 3 in comparison with the cheaper methods. It can be seen that most methods can correctly assign the same GM as the CCSD(T) benchmark, with the exception of the two ECP cases and the M06-2X functional. These results are also summarized in Table 3.

Once again, the ideal choice would be the scaled variants of the MP2 method, with special attention to SOS-MP2, which showed the overall lowest MAE. Among the DFT functionals, TPSSh and PBE0 are the best choices since their associated MAEs are considerably lower than for B3LYP, showing much more correspondences with the minima existing in the benchmark PES (# matches). Including an ECP calculation using the best functional (PBE0) did not lead to a drastic increase in the MAE, but it changed the energetic ordering,

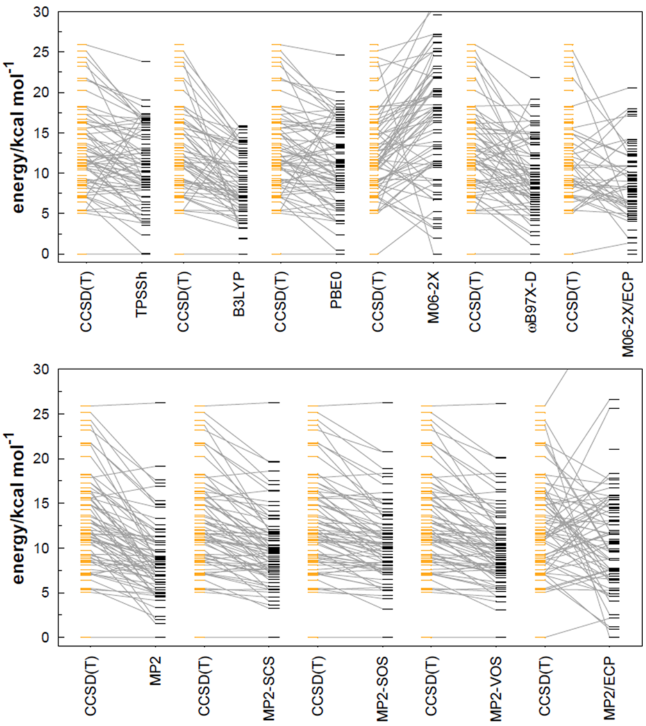

Figure 3. Comparisons between the homotops of Al_4Si_7 between benchmark CCSD(T)/CBS and lower level methods. The color scheme is the same as in Figure 2.

Table 3. Results for Al_4Si_7[a]

method	# matches	MAE	ΔGM	NSR
TPSSh	70	3.31	0.00	1
B3LYP	60	4.37	0.00	1
PBE0	71	3.07	0.00	1
M06-2X	66	5.72	5.25	8
ωB97X-D	65	4.08	0.00	1
PBE0/ECP	41	3.75	1.34	3
MP2	74	4.10	0.00	1
SCS-MP2	74	2.93	0.00	1
SOS-MP2	74	2.36	0.00	1
VOS-MP2	74	2.71	0.00	1
MP2/ECP	65	5.03	2.14	4

[a] Energies are given in kcal mol^{-1}.

such that the GM in this case is not the same GM of the benchmark database. Even so, the NSR is only 3, and thus it is still a useful approach for a global optimization.

3.4. P_{11}^+.

Several cationic phosphorus clusters have been produced experimentally in the gas phase by laser vaporization[62,63] and their abundances measured by time-of-flight mass spectrometry. The odd-sized P_n^+ cations show an even number of electrons, and almost all cases with n<15 show strong peaks in the spectra.[63] We have applied our approach to the P_{11}^+ cluster, whose covalent bonds make it a quite different system if compared to the previous ones.

Due to its molecular character, several van der Waals minima composed by one or more P_2 units can be observed: these can be described as $P_{n-2x}^+ + xP_2$. Nevertheless, the deepest minima in the PES correspond to fully bonded P_{11}^+. The number of nonequivalent local energy minima in this PES is too high possibly due to innumerable orientations of van der Waals interactions. In this case, our benchmark set consists of 184 local minima, and the CCSD(T) energies took 938 days of single CPU time (note that within the set of elements studied in this work, P has the largest number of electrons).

The results are shown in Table 4 and Figure 4, from where it is seen that the ωB97X-D functional was the most suited for a global optimization since it shows the same GM as the benchmark set and could therefore be used in an exploration that yielded only one structure for further refinement at the improved level. This should not be a surprise since the dispersion corrections of this functional should help describing the many van der Waals minima present in this system. A good result is also obtained with TPSSh, although this functional showed a slightly higher MAE value. Although the PBE0

Table 4. Results for P_{11}^+[a]

method	# matches	MAE	ΔGM	NSR
TPSSh	73	11.11	0.00	1
B3LYP	48	16.38	2.79	3
PBE0	74	6.77	NM[b]	
M06-2X	81	13.77	0.15	2
ωB97X-D	66	10.23	0.00	1
ωB97X-D/ECP	62	18.06	14.84	5
MP2	184	15.32	0.00	1
SCS-MP2	184	19.12	0.00	1
SOS-MP2	184	19.55	2.23	3
VOS-MP2	184	21.20	0.85	2
MP2/ECP	88	32.22	27.09	102

[a] Energies are given in kcal mol^{-1}. [b] No match (NM): the global minimum at the benchmark level has no matching structure at this approach.

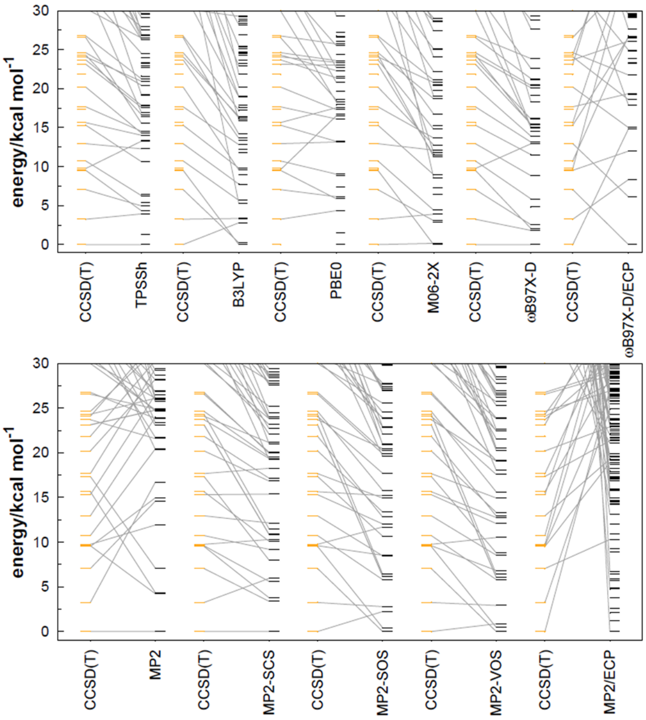

Figure 4. Comparisons between the minima of P_{11}^+ with several low-level approaches against the benchmark CCSD(T)/CBS calculations. The color scheme is the same as in Figure 2. A plot showing the full energy range and all minima obtained can be found in the Supporting Information.

functional yielded the lowest MAE, it did not show any structure that could be matched to the benchmark GM. Since this system has so many minima, there is a chance that the PBE0 PES does present the correct minimum, but it was not generated in our database. Consequently, this should not be taken as a serious problem for using PBE0 in general global optimizations. The B3LYP and M06-2X functionals are also not bad choices since their third and second minima (respectively) can already be matched to the correct one. Employing the best functional (ωB97X-D) with an effective core potential shows a worsening in the results but would still be acceptable for a global optimization in which the five lowest energy structures are selected for posterior refinement.

This system was the only one in which all scaled variants of the MP2 method were not the best choices overall. As it can be seen, only the regular MP2 and SCS-MP2 show the correct GM structure, and their MAE are higher than the DFT calculations. The fact that there are many van der Waals structures of the $P^+_{n-2x} + xP_2$ type could help explain these results. For structures of this type, long-range nondynamic correlation should be important. However, all MP2 variants used in this work scale down (or even nullify) the correlation effects of electrons with the same spin (SS), which is precisely more connected with nondynamic correlation.[56] This is likely to lead to an unbalanced energetic treatment of many of these structures, which is then reflected in the MAE. Note that the highest values of the MAE correspond to SOS-MP2 and VOS-MP2, the only two variants in which the SS contribution is absent. The use of an ECP with the MP2 method drastically deteriorates the results, more than doubling the MAE.

4. CONCLUDING REMARKS

In this work, we have explored several minima in the PESs of nanoalloys by utilizing 12 distinct electronic structure approaches for trying to shed light on the viability of using a lower level method to perform global optimizations and obtain the most probable structures produced experimentally. For this, we have chosen different cluster types, including alkali, metallic, molecular, and also pure and alloy cases.

Perhaps the most comforting conclusion reached here is that, if the global optimization with a particular functional can yield a handful of low energy structures (not only the global minimum) for further refinement with a higher level method, the true global minimum of an accurate PES is very likely to be obtained. Such approach is often used in the literature, and the geometries obtained are used for a posterior calculation of relevant properties, such as vibrational frequencies, ionization potential, and so on. If the geometrical structure was correctly obtained by the global optimization method, the results will be useful for guiding the design of new nanoclusters with interesting applications, and therefore the results of the present work are motivating.

Specifically, within the five tested functionals, TPSSh with the pcseg-1 basis set has shown to be the best DFT method for the global optimization, with excellent results for all cases here analyzed. Although we have not presented an exhaustive list of tested functionals, the variety of the studied systems gives us an indication that TPSSh/pcseg-1 could be a reliable methodology in a wider context. It is also found that, although the use of an effective core potential worsens the results, it shows fairly good features with the functionals explored here and may be applicable if about 10 lowest energy structures are to be further refined.

Although MP2 approaches are not the standard choice for global optimizations, they have recently also been the choice for specific cases.[54,55] Within this approach, we have found that the scaled variants provide the best results overall, except for P^+_{11} due to its large number of van der Waals structures. The inclusion of an effective core potential in the unscaled MP2 method has caused a more drastic worsening on the results than its inclusion on the DFT functionals, judging by the ΔGM value.

■ ASSOCIATED CONTENT

Supporting Information

The Supporting Information is available free of charge on the ACS Publications website at DOI: 10.1021/acs.jpca.9b09309.

> Cartesian coordinates and energies for all structures in the benchmark databases (CCSD(T)/CBS//MP2/VDZ) and the graphs of this manuscript showing all energy minima (ZIP)

■ AUTHOR INFORMATION

Corresponding Authors

*E-mail: brenogalvao@gmail.com (B.R.L.G.).
*E-mail: lpviegas@gmail.com (L.P.V.).

ORCID

Breno R. L. Galvão: 0000-0002-4184-2437
Luís P. Viegas: 0000-0003-2312-990X

Present Address

§Present address: Coimbra Chemistry Center and Chemistry Department, University of Coimbra, 3004-535 Coimbra, Portugal.

Notes

The authors declare no competing financial interest.

■ ACKNOWLEDGMENTS

We are thankful for the financial support provided by the Coordenação de Aperfeiçoamento de Pessoal de Nível Superior - Brasil (CAPES) - Finance Code 001, Conselho Nacional de Desenvolvimento Científico e Tecnológico (CNPq), grants 403352/2016-9 and 305469/2018-5, and Fundação de Amparo à Pesquisa do estado de Minas Gerais (FAPEMIG), grant CEX - APQ-00071-15. B.R.L.G. is also thankful to Rede Mineira de Química (RQ-MG). L.P.V. also acknowledges financial support from the AIAS-COFUND Marie Curie program (through the EU's FP7 for Research, Technological Development and Demonstration under Grant Agreement No. 609033) and Prof. Frank Jensen for providing access to the computational resources.

■ REFERENCES

(1) Tyo, E. C.; Vajda, S. Catalysis by clusters with precise numbers of atoms. *Nat. Nanotechnol.* **2015**, *10*, 577.

(2) Klębowski, B.; Depciuch, J.; Parlińska-Wojtan, M.; Baran, J. Applications of noble metal-based nanoparticles in medicine. *Int. J. Mol. Sci.* **2018**, *19*, 4031.

(3) Shayeghi, A.; Johnston, R. L.; Schäfer, R. Communication: Global minimum search of Ag_{10}^+ with molecular beam optical spectroscopy. *J. Chem. Phys.* **2014**, *141*, 181104.

(4) Wales, D. J.; Doye, J. P. K. Global optimization by basin-hopping and the lowest energy structures of Lennard-Jones clusters containing up to 110 Atoms. *J. Phys. Chem. A* **1997**, *101*, 5111−5116.

(5) Johnston, R. L. Evolving better nanoparticles: Genetic algorithms for optimising cluster geometries. *J. Chem. Soc. Dalton Trans.* **2003**, 4193−4207.

(6) Ahuja, P.; Molayem, M.; Gadre, S. R. Electrostatics-assisted building-up procedure for capturing energy minima of metal clusters: Test case of Ag_n clusters. *J. Phys. Chem. A* **2019**, *123*, 7872−7880.

(7) Alexandrova, A. N.; Boldyrev, A. I.; Fu, Y.-J.; Yang, X.; Wang, X.-B.; Wang, L.-S. Structure of the $Na_xCl_{x+1}^-$ (x=1−4) clusters via ab initio genetic algorithm and photoelectron spectroscopy. *J. Chem. Phys.* **2004**, *121*, 5709−5719.

(8) Chuang, F.-C.; Wang, C. Z.; Ho, K. H. Structure of neutral aluminum clusters $Al_n(2 \leqslant n \leqslant 23)$: Genetic algorithm tight-binding calculations. *Phys. Rev. B* **2006**, *73*, 125431.

(9) Huang, W.; Pal, R.; Wang, L.-M.; Zeng, X. C.; Wang, L.-S. Isomer identification and resolution in small gold clusters. *J. Chem. Phys.* **2010**, *132*, No. 054305.

(10) Dieterich, J. M.; Hartke, B. OGOLEM: Global cluster structure optimisation for arbitrary mixtures of flexible molecules. A multi-scaling, object-oriented approach. *Mol. Phys.* **2010**, *108*, 279−291.

(11) Drebov, N.; Ahlrichs, R. Structures of Al_n, its anions and cations up to n=34: A theoretical investigation. *J. Chem. Phys.* **2010**, *132*, 164703.

(12) Heiles, S.; Johnston, R. L.; Schäfer, R. Bismuth-doped Tin clusters: experimental and theoretical studies of neutral Zintl analogues. *J. Phys. Chem. A* **2012**, *116*, 7756−7764.

(13) Heiles, S.; Logsdail, A. J.; Schäfer, R.; Johnston, R. L. Dopant-induced 2D-3D transition in small Au-containing clusters: DFT-global optimisation of 8-atom Au-Ag nanoalloys. *Nanoscale* **2012**, *4*, 1109−1115.

(14) Forck, R. M.; Dieterich, J. M.; Pradzynski, C. C.; Huchting, A. L.; Mata, R. A.; Zeuch, T. Structural diversity in sodium doped water trimers. *Phys. Chem. Chem. Phys.* **2012**, *14*, 9054−9057.

(15) Götz, D. A.; Heiles, S.; Johnston, R. L.; Schäfer, R. Note: Gas phase structures of bare Si_8 and Si_{11} clusters from molecular beam electric deflection experiments. *J. Chem. Phys.* **2012**, *136*, 186101.

(16) Shayeghi, A.; Johnston, R. L.; Schäfer, R. Evaluation of photodissociation spectroscopy as a structure elucidation tool for isolated clusters: a case study of Ag_4^+ and Au_4^+. *Phys. Chem. Chem. Phys.* **2013**, *15*, 19715−19723.

(17) Heiles, S.; Johnston, R. L. Global optimization of clusters using electronic structure methods. *Int. J. Quantum Chem.* **2013**, *113*, 2091−2109.

(18) Götz, D. A.; Shayeghi, A.; Johnston, R. L.; Schwerdtfeger, P.; Schäfer, R. Influence of spin-orbit effects on structures and dielectric properties of neutral lead clusters. *J. Chem. Phys.* **2014**, *140*, 164313.

(19) Farrow, M. R.; Chow, Y.; Woodley, S. M. Structure prediction of nanoclusters; a direct or a pre-screened search on the DFT energy landscape? *Phys. Chem. Chem. Phys.* **2014**, *16*, 21119−21134.

(20) Shayeghi, A.; Heard, C. J.; Johnston, R. L.; Schäfer, R. Optical and electronic properties of mixed Ag-Au tetramer cations. *J. Chem. Phys.* **2014**, *140*, No. 054312.

(21) Götz, D. A.; Shayeghi, A.; Johnston, R. L.; Schwerdtfeger, P.; Schäfer, R. Structural evolution and metallicity of lead clusters. *Nanoscale* **2016**, *8*, 11153−11160.

(22) Paiva, M. A. M.; Peluzo, B. M. T. C.; Belchior, J. C.; Galvão, B. R. L. Structure and stability of neutral Al-Mg nanoclusters up to 55 atoms. *Phys. Chem. Chem. Phys.* **2016**, *18*, 31579−31585.

(23) Silva, M. X.; Silva, F. T.; Galvão, B. R. L.; Braga, J. P.; Belchior, J. C. A genetic algorithm survey on closed-shell atomic nitrogen clusters employing a quantum chemical approach. *J. Mol. Model.* **2018**, *24*, 196.

(24) Raghavachari, K.; Trucks, G. W.; Pople, J. A.; Head-Gordon, M. A fifth-order perturbation comparison of electron correlation theories. *Chem. Phys. Lett.* **1989**, *157*, 479.

(25) Piecuch, P.; Kucharski, S. A.; Kowalski, K.; Musiał, M. Efficient computer implementation of the renormalized coupled-cluster methods: The R-CCSD[T], R-CCSD(T), CR-CCSD[T], and CR-CCSD(T) approaches. *Comput. Phys. Commun.* **2002**, *149*, 71−96.

(26) Bentz, J. L.; Olson, R. M.; Gordon, M. S.; Schmidt, M. W.; Kendall, R. A. Coupled cluster algorithms for networks of shared memory parallel processors. *Comput. Phys. Commun.* **2007**, *176*, 589−600.

(27) Olson, R. M.; Bentz, J. L.; Kendall, R. A.; Schmidt, M. W.; Gordon, M. S. A novel approach to parallel coupled cluster calculations: Combining distributed and shared memory techniques for modern cluster based systems. *J. Chem. Theory Comput.* **2007**, *3*, 1312−1328.

(28) Møller, C.; Plesset, M. S. Note on an approximation treatment for many-electron systems. *Phys. Rev.* **1934**, *46*, 618.

(29) Dunning, T. H., Jr.; Peterson, K. A.; Wilson, A. K. Gaussian basis sets for use in correlated molecular calculations. X. The atoms aluminum through argon revisited. *J. Chem. Phys.* **2001**, *114*, 9244.

(30) Hay, P. J.; Wadt, W. R. Ab initio effective core potentials for molecular calculations. Potentials for the transition metal atoms Sc to Hg. *J. Chem. Phys.* **1985**, *82*, 270.

(31) Wadt, W. R.; Hay, P. J. Ab initio effective core potentials for molecular calculations. Potentials for main group elements Na to Bi. *J. Chem. Phys.* **1985**, *82*, 284.

(32) Hay, P. J.; Wadt, W. R. Ab initio effective core potentials for molecular calculations. Potentials for K to Au including the outermost core orbitals. *J. Chem. Phys.* **1985**, *82*, 299.

(33) Grimme, S. Improved second-order Møller-Plesset perturbation theory by separate scaling of parallel- and antiparallel-spin pair correlation energies. *J. Chem. Phys.* **2003**, *118*, 9095.

(34) Jung, Y.; Lochan, R. C.; Dutoi, A. D.; Head-Gordon, M. Scaled opposite-spin second order Møller-Plesset correlation energy: an economical electronic structure method. *J. Chem. Phys.* **2004**, *121*, 9793.

(35) Varandas, A. J. C. Spin-component-scaling second-order Møller-Plesset theory and its variants for economical correlation energies: Unified theoretical interpretation and use for quartet N_3. *J. Chem. Phys.* **2010**, *133*, No. 064104.

(36) Varandas, A. J. C. Extrapolating to the one-electron basis-set limit in electronic structure calculations. *J. Chem. Phys.* **2007**, *126*, 244105.

(37) Varandas, A. J. C.; Pansini, F. N. N. Narrowing the error in electron correlation calculations by basis set re-hierarchization and use of the unified singlet and triplet electron-pair extrapolation scheme: Application to a test set of 106 systems. *J. Chem. Phys.* **2014**, *141*, 224113.

(38) Pansini, F. N. N.; Neto, A. C.; Varandas, A. J. C. Extrapolation of Hartree-Fock and multiconfiguration selfconsistent-field energies to the complete basis set limit. *Theor. Chem. Acc.* **2016**, *135*, 261.

(39) Staroverov, V. N.; Scuseria, G. E.; Tao, J.; Perdew, J. P. Comparative assessment of a new nonempirical density functional: Molecules and hydrogen-bonded complexes. *J. Chem. Phys.* **2003**, *119*, 12129.

(40) Becke, A. D. Density-functional thermochemistry. III. The role of exact exchange. *J. Chem. Phys.* **1993**, *98*, 5648.

(41) Stephens, P. J.; Devlin, F. J.; Chabalowski, C. F.; Frisch, M. J. Ab initio calculation of vibrational absorption and circular dichroism spectra using density functional force fields. *J. Phys. Chem.* **1994**, *98*, 11623−11627.

(42) Hertwig, R. H.; Koch, W. On the parameterization of the local correlation functional. What is Becke-3-LYP? *Chem. Phys. Lett.* **1997**, *268*, 345.

(43) Adamo, C.; Barone, V. Toward chemical accuracy in the computation of NMR shieldings: the PBE0 model. *Chem. Phys. Lett.* **1998**, *298*, 113.

(44) Adamo, C.; Barone, V. Toward reliable density functional methods without adjustable parameters: The PBE0 model. *J. Chem. Phys.* **1999**, *110*, 6158.

(45) Zhao, Y.; Truhlar, D. G. The M06 suite of density functionals for main group thermochemistry, thermochemical kinetics, non-covalent interactions, excited states, and transition elements: Two new functionals and systematic testing of four M06-class functionals and 12 other functionals. *Theor. Chem. Acc.* **2008**, *120*, 215−241.

DOI: 10.1021/acs.jpca.9b09309

(46) Chai, J.-D.; Head-Gordon, M. Long-range corrected hybrid density functionals with damped atomatom dispersion corrections. *Phys. Chem. Chem. Phys.* **2008**, *10*, 6615−6620.

(47) Perdew, J. P.; Schmidt, K. *Density functional theory and its application to materials*; Van Doren, V., Van Alsenoy, C., Geerlings, P., Eds.; AIP: Melville, NY, 2001; pp 1−20.

(48) Perdew, J. P.; Ruzsinszky, A.; Tao, J.; Staroverov, V. N.; Scuseria, G. E.; Csonka, G. I. Prescription for the design and selection of density functional approximations: More constraint satisfaction with fewer fits. *J. Chem. Phys.* **2005**, *123*, No. 062201.

(49) Jensen, F. Unifying general and segmented contracted basis sets. Segmented polarization consistent basis sets. *J. Chem. Theory Comput.* **2014**, *10*, 1074−1085.

(50) Schmidt, M. W.; Baldridge, K. K.; Boatz, J. A.; Elbert, S. T.; Gordon, M. S.; Jensen, J. H.; Koseki, S.; Matsunaga, N.; Nguyen, K. A.; Su, S.; et al. General atomic and molecular electronic structure system. *J. Comput. Chem.* **1993**, *14*, 1347.

(51) Viegas, L. P. Exploring the reactivity of hydrofluoropolyethers toward OH through a cost-effective protocol for calculating multiconformer transition state theory rate constants. *J. Phys. Chem. A* **2018**, *122*, 9721−9732.

(52) Vásquez-Pérez, J. M.; Martínez, G. U. G.; Köster, A. M.; Calaminici, P. The discovery of unexpected isomers in sodium heptamers by Born−Oppenheimer molecular dynamics. *J. Chem. Phys.* **2009**, *131*, 124126.

(53) Marques, J. M. C.; Llanio-Trujillo, J. L.; Abreu, P. E.; Pereira, F. B. How different are two chemical structures? *J. Chem. Inf. Model.* **2010**, *50*, 2129−2140.

(54) Silva, F. T.; Galvão, B. R. L.; Voga, G. P.; Silva, M. X.; Rodrigues, D. D. C.; Belchior, J. C. Exploring the MP2 energy surface of nanoalloy clusters with a genetic algorithm: Application to sodium-potassium. *Chem. Phys. Lett.* **2015**, *639*, 135−141.

(55) Silveira, A. D. P.; Gomes, A. C. R.; Galvão, B. R. L. Structural and homotop optimization of neutral Al-Si nanoclusters. *Phys. Chem. Chem. Phys.* **2018**, *20*, 17464−17470.

(56) Grimme, S.; Goerigk, L.; Fink, R. F. Spin-component-scaled electron correlation methods. *Wiley Interdiscip. Rev.: Comput. Mol. Sci.* **2012**, *2*, 886−906.

(57) Grimme, S. Density functional theory with London dispersion corrections. *Wiley Interdiscip. Rev.: Comput. Mol. Sci.* **2011**, *1*, 211−228.

(58) Jellinek, J.; Krissinel, E. B. Ni_nAl_m alloy clusters: Analysis of structural forms and their energy ordering. *Chem. Phys. Lett.* **1996**, *258*, 283−292.

(59) Orlov, A. O.; Amlani, I.; Bernstein, G. H.; Lent, C. S.; Snider, G. L. Realization of a functional cell for quantum-dot cellular automata. *Science* **1997**, *277*, 928−930.

(60) Knight, W. D.; Clemenger, K.; de Heer, W. A.; Saunders, W. A.; Chou, M. Y.; Cohen, M. L. Electronic shell structure and abundances of sodium clusters. *Phys. Rev. Lett.* **1984**, *52*, 2141−2143.

(61) Jellinek, J.; Acioli, P. H. Magnesium clusters: Structural and electronic properties and the size-induced nonmetal-to-metal transition. *J. Phys. Chem. A* **2002**, *106*, 10919−10925.

(62) Huang, R.; Li, H.; Lin, Z.; Yang, S. Experimental and theoretical studies of small homoatomic phosphorus clusters. *J. Phys. Chem.* **1995**, *99*, 1418−1423.

(63) Liu, Z.-y.; Huang, R.-b.; Zheng, L.-s. Bare phosphorus and binary phosphide cluster ions generated by laser ablation. *Z. Phys. D: At., Mol. Clusters* **1996**, *38*, 171−177.

DOI: 10.1021/acs.jpca.9b09309
J. Phys. Chem. A XXXX, XXX, XXX−XXX